On the Nature of the Bursting X-Ray Pulsar GRO J1744-28

Steven J. Sturner[1] & Charles D. Dermer
E. O. Hulburt Center for Space Research, Code 7653,
Naval Research Laboratory, Washington, DC 20375-5352

ABSTRACT

The unusual properties of the bursting X-ray pulsar GRO J1744-28 are explained in terms of a low-mass X-ray binary system consisting of an evolved stellar companion transferring mass through Roche-lobe overflow onto a neutron star, implying that the inclination of the system is $\lesssim 18^\circ$. Interpretation of the QPO at frequency $\nu_{\rm QPO} = 40$ Hz using the beat-frequency model of Alpar & Shaham and the measured period derivative $\dot{P}$ with the Ghosh & Lamb accretion-torque model implies that the persistent X-ray luminosity of the source is approximately equal to the Eddington luminosity and that the neutron star has a surface equatorial magnetic field $B_{\rm eq} \cong 2 \times 10^{10}\ (\nu_{\rm QPO}/40\ {\rm Hz})^{-1}$ G for standard neutron star parameters. This implies a distance to GRO J1744-28 of $\cong 5\ (\nu_{\rm QPO}/40\ {\rm Hz})^{1/6} b^{1/2}$ kpc, where $b < 1$ is a correction factor that depends on the orientation of the neutron star.

Subject headings: accretion — stars:binary:close — stars:neutron — pulsars:individual (GRO J1744-28) — X-rays:bursts

1. Introduction

GRO J1744-28, a 2.1 Hz X-ray pulsar with unusual bursting properties, was discovered on 2 December 1995 in the direction of the Galactic Center with the Burst and Transient Source Experiment (BATSE) on the *Compton Gamma Ray Observatory* (Kouveliotou et al. 1996a; Finger et al. 1996a). The source initially bursted about every 3 minutes, then declined in frequency to about 30 per day for the first month, after which it increased in frequency to about 40 per day in the period 8-18 January 1996 (Fishman et al. 1996). The *Rossi X-ray Timing Explorer* (*RXTE*) (Swank et al. 1996) localized the source to galactic

[1]NRL/NRC Research Associate

coordinates $l = +0.02°, b = +0.3°$. Both the persistent and bursting X-ray emissions show pulsations with a 0.467 s period (Kouveliotou et al. 1996b) and have similar hard X-ray and soft gamma-ray spectra (Briggs et al. 1996; Strickman et al. 1996) with a color temperature ≈ 10 keV, characteristic of X-ray pulsars.

In this *Letter*, we show that the observations are best explained by a neutron star accreting matter through Roche lobe overflow from an evolved low-mass stellar companion. We derive values for the magnetic field stength and accretion luminosity by noting that the beat frequency model (Alpar & Shaham 1985) for QPOs and the accretion-torque model (Ghosh & Lamb 1979) for the pulsar spin-up rate separately imply relations between these two quantities. The size and temperature of the polar-cap hot spot are determined. The observed pulse fraction is used to constrain the orientation and geometry of the neutron star, and to derive the distance to the system from the calculated luminosity.

2. Nature of the Stellar Companion

The present mass $M_* = M_*(i)$ of the neutron star's stellar companion can be calculated as a function of orbital inclination angle i using the measured (Finger, Wilson, & van Paradijs 1996b) value of the mass function

$$f_{\rm x} = 1.31 \times 10^{-4}\ M_\odot = \frac{(M_* \sin i)^3}{(M_{\rm NS} + M_*)^2}. \tag{1}$$

The solution to equation (1) is plotted in Figure 1, assuming a neutron star mass $M_{\rm NS} = 1.4 M_{1.4}\ M_\odot$ with $M_{1.4} = 1$. We find that $M_*(i) \lesssim 1 M_\odot$ unless $i \lesssim 6°$. The mean separation between the neutron star and its companion is given by

$$a(i) = a_{\rm x} \sin i\ \left[\frac{M_{\rm NS} + M_*(i)}{M_*(i) \sin i}\right], \tag{2}$$

where $a_{\rm x} \sin i = 1.12\ R_\odot = 7.76 \times 10^{10}$ cm (Finger et al. 1996b). As can be seen in Figure 1, the values of $a(i)$ range from $\sim 25\ R_\odot$ for $i > 5°$ to $\sim 80\ R_\odot$ for $i = 1°$.

Mass transfer in a low-mass system occurs through Roche-lobe overflow rather than via a stellar wind (e.g., Verbunt 1990). Given $M_*(i)$ and $a(i)$, the average radius of the Roche lobe around the stellar companion, $R_{\rm RL}(i)$, can be determined from the expressions

$$R_{\rm RL}(i) \simeq a(i)\,\{0.38 + 0.2 \log[M_*(i)/M_{\rm NS}]\}\ ; \qquad M_* \gtrsim M_{\rm NS}, \tag{3a}$$

$$\simeq 0.46\ a(i) \left[\frac{M_*(i)}{M_{\rm NS} + M_*(i)}\right]^{1/3}\ ; \qquad M_* \lesssim M_{\rm NS} \tag{3b}$$

(e. g. Verbunt 1990). $R_{\rm RL}(i)$ is plotted in Figure 1 and varies from 4 $R_\odot$ at $i = 90^\circ$ to 40 $R_\odot$ at $i = 1^\circ$. Such sizes greatly exceed the radii of main sequence stars with masses $M_*(i)$, which we also plot in Figure 1 (e.g., Mihalas & Binney 1982). Accretion via Roche lobe overflow can occur however if the companion star has evolved off the main sequence, which is possible within the lifetime of the Galaxy for stars with initial masses $\gtrsim 1.0\ M_\odot$. A companion with a current mass $> 1\ M_\odot$ requires that the system be nearly face-on, with $i \lesssim 6^\circ$, but mass transfer to the neutron star could have decreased the companion's present mass even if its initial mass was $> 1\ M_\odot$.

The evolved companion star must presently have a radius $R_* \gtrsim R_{\rm RL}(i)$. The radii of evolved low-mass stars depend mainly on their helium core masses (Webbink, Rappaport, & Savonije 1983). We can use the relations of Webbink et al. (1983) to place a lower limit on the present mass of the companion by requiring it to be larger than the helium core mass. In the inset to Figure 1, we plot the stellar radius of an evolved companion versus its helium core mass as well as the Roche lobe radius versus stellar mass. We find that the smallest helium core mass which allows for Roche-lobe overflow in GRO J1744-28 is $\sim 0.22\ M_\odot$. Thus $M_* \gtrsim 0.22\ M_\odot$ and therefore $i < 18^\circ$. The chance probablity for viewing the system with this inclination is 1 in ∼20. Also shown in Figure 1 is the no-eclipse condition assuming that $R_* = R_{\rm RL}$. This restricts $i \lesssim 80^\circ$, which is less constraining than the above considerations.

3. Accretion Dynamics

The Alfvén radius for spherical accretion, obtained by balancing accretion and magnetic pressure, is given by

$$R_{\rm A} = 1.9 \times 10^8\ \mu_{30}^{4/7}\ M_{1.4}^{1/7}\ (L_{38}\ R_6)^{-2/7}\ \ {\rm cm}, \tag{4}$$

where L_{38} is the pulsar luminosity in units of 10^{38} erg s^{-1}, $\mu = B_{\rm eq} R_{\rm NS}^3 = 10^{30}\mu_{30}$ G-cm^3 is the neutron star magnetic moment ($B_{\rm eq}$ is the surface equatorial field strength), and $10^6 R_6$ cm is the neutron star radius. The corotation radius, where the Keplerian and rigid body rotation velocities are equal, is given by $R_{\rm co} = (GM_{\rm NS})^{1/3}(P/2\pi)^{2/3} = 1.0 \times 10^8\ M_{1.4}^{1/3}$ cm using $P = 0.467$ s for GRO J1744-28. The transition from Keplerian motion to corotation with the neutron star magnetosphere occurs at $r = \eta R_{\rm A}$, where $\eta \approx 1$. The requirement that $\eta R_{\rm A} < R_{\rm co}$ for acretion to take place yields $B_{\rm eq} \lesssim 3.3 \times 10^{11}\ L_{38}^{1/2}\ M_{1.4}^{1/3}\ R_6^{-5/2} \eta^{-7/4}$ G. Requiring magnetic confinement of the hot plasma in the accretion column sets a lower limit on the surface polar magnetic field strength $B_{\rm p}$ ($= 2B_{\rm eq}$ for a dipole magnetic field) through the expression $B_{\rm p}^2/8\pi \gtrsim L/A_{\rm pc}c \approx \sigma_{\rm SB}T^4/c$, where we use the blackbody radiation

formula to estimate the polar cap area $A_{\rm pc}$. Thus $B_{\rm p} \gtrsim 2.9 \times 10^9\ T_{10}^2$ G, where T_{10} is the effective temperature in units of 10 keV.

A more precise estimate for magnetic field strength and accretion luminosity can be obtained by interpreting the measured QPO frequency using the beat frequency model of Alpar & Shaham (1985), and the pulsar spin-up rate from the Ghosh & Lamb (1979) accretion-torque model. Zhang et al. (1996) report a QPO at frequency $\nu_{\rm QPO} = 40$ Hz with integrated power (uncorrected for deadtime) under the 27 Hz FWHM Lorentzian equal to 5.6% of the total power. Although the width of this QPO is somewhat larger than those typically measured in low mass X-ray binaries, with FWHM widths $\lesssim 0.5$ the centroid frequencies (see, e.g., van der Klis 1995), we still assume that $\nu_{\rm QPO}$ can be interpreted as the beat frequency between the Keplerian frequency $\nu_{\rm K} = (GM_{\rm NS})^{1/2}(2\pi)^{-1}r^{-3/2}$ at $r = \eta R_{\rm A}$ and the neutron star's rotation frequency $\nu_{\rm NS}$ (Alpar & Shaham 1985). Less significant peaks in the power spectrum are also found at 20 and 60 Hz, and we cannot exclude that the 40 Hz peak is a harmonic of the 20 Hz peak but with larger amplitude. This implies

$$B_{\rm eq} = 1.1 \times 10^{10}\ \tilde{\nu}^{-7/6}\ L_{38}^{1/2}\ M_{1.4}^{1/3}\ R_6^{-5/2}\ \eta^{-7/4}\ {\rm G} \tag{5}$$

and

$$\eta R_{\rm A} = 1.4 \times 10^7\ \tilde{\nu}^{-2/3}\ M_{1.4}^{1/3}\ {\rm cm}, \tag{6}$$

where we define $\tilde{\nu} = (\nu_{\rm QPO} + \nu_{\rm NS})/40$ Hz.

An expression for the period derivative of a disk-fed X-ray pulsar as a function of neutron star properties was derived by Ghosh & Lamb (1979). Substituting equation (5) into their equation (15) gives

$$-\dot{P} = 2.6 \times 10^{-5}\ \tilde{\nu}^{-1/3}\ L_{38}\ M_{1.4}^{-1/3}\ R_6\ I_{45}^{-1}\ \eta^{-1/2}\ f(\omega_{\rm s})\ \ {\rm s\ yr}^{-1}, \tag{7}$$

where I_{45} is the neutron star moment of inertia in units of 10^{45} g-cm^2, and $f(\omega_s)$, proportional to the dimensionless torque function (see Ghosh & Lamb 1979; Wang 1995), is a function of the fastness parameter $\omega_s = (\eta R_A/R_{\rm co})^{3/2}$. For GRO J1744-28, $\omega_{\rm s} \cong 0.05\ \tilde{\nu}^{-1}\ \ll 1$, implying $f(\omega_s) \approx 0.9$. The observed period derivative is $\dot{P} = -5.95 \times 10^{-5}$ s yr^{-1} (Finger et al. 1996b), which could however be different than the value at the epoch 18-19 January 1996 when *RXTE* measured the 40 Hz QPO. In terms of the Eddington luminosity $L_{\rm Edd} = 1.76 \times 10^{38}\ M_{1.4}$ erg s^{-1}, we obtain a pulsar luminosity given by

$$L/L_{\rm Edd} \cong 1.4\ \eta^{1/2}\ \tilde{\nu}^{1/3}\ M_{1.4}^{-2/3}\ R_6^{-1}\ I_{45}\ . \tag{8}$$

Substituting equation (8) into (5), we obtain

$$B_{\rm eq} \cong 1.8 \times 10^{10}\ \eta^{-3/2}\ \tilde{\nu}^{-1}\ M_{1.4}^{1/2}\ R_6^{-3}\ I_{45}^{1/2}\ {\rm G}\ . \tag{9}$$

The derived value for the magnetic field at the neutron star's equator depends only upon quantities intrinsic to the neutron star and details of the accretion process, and is bracketed by our estimates given above. We suggest a search with *RXTE* or *ASCA* for cyclotron absorption features with a fundamental energy at $\sim$ 1-2 keV; note that a larger field is inferred if one assumes that the 20 Hz peak in the power spectrum is the fundamental. The magnetic field given by equation (9) does not conflict with OSSE observations, which show no evidence for cyclotron features at > 40 keV (Strickman et al. 1996).

4. X-Ray Pulsar Geometry

Equation (6) for the stopping radius yields a size of the polar-cap hot spot if we assume that its area is determined by the footprints of those magnetic field lines that cross the magnetic equator at $r = \eta R_{\rm A}$. For an assumed dipolar magnetic field geometry, $\sin^2\theta_{\rm m}/r =$ constant, where $\theta_{\rm m}$ is the magnetic colatitude. Thus for an aligned rotator $\theta_{\rm pc} = \arcsin\left[0.26\ \tilde{\nu}^{1/3}\ M_{1.4}^{-1/6}\ R_6^{1/2}\right] \cong 15^\circ$, although the hot spot size of an oblique rotator could be smaller if the matter does not accrete uniformly onto the polar cap. The hot-spot size and source luminosity from equation (8) imply an effective temperature of $\cong 4.9\ \eta^{1/8}\tilde{\nu}^{1/12}M_{1.4}^{1/12}R_6^{-3/4}I_{45}^{1/4}$ keV. This is in reasonable agreement with the values of 6 and 14 keV for the blackbody temperature and e-folding energy reported by BATSE (Briggs et al. 1996) and *RXTE* (Swank et al. 1996), respectively.

BATSE reports a pulse fraction in the persistent emission of 40% in the 25-45 keV band (Finger et al. 1996a), whereas smaller energy-dependent values are measured with *RXTE* for the band between 3 and 12 keV (Zhang 1996). These pulsations are probably due to projection effects of the X-ray hot spots on the rotating neutron star. Figure 2 shows the various orientations and obliquenesses that produce pulse fractions of 20, 30, and 40% calculated from a purely geometric model consisting of two identical uniformly-emitting polar caps. The large luminosities radiated from a small area may produce a fan-beam radiation pattern, but are not considered here. We include shadowing effects from the neutron star but not from the accretion column. A large range of angles are permitted for a given pulse fraction. During the bursting episodes, the flux increases by a factor of 2-8 whereas the spectrum remains nearly identical (a relative excess below 3-4 keV is seen during outbursts by *RXTE*; Zhang 1996). Interpreting the increase in flux as due to an increase in emitting area, we predict that the pulse fraction should decrease by an amount dependent on α (see inset to Figure 2). The energy-dependence of the pulse fraction could be a consequence of thermal stratification, with the hotter inner regions therefore showing a larger pulse fraction.

The 2-100 keV energy flux reported by *RXTE* at epoch 18-19 January 1996 (Swank et al. 1996) is $\phi = 2 \times 10^{-7}$ ergs cm^{-2} s^{-1} for the persistent emission. The luminosity from equation (8) then implies a distance to GRO J1744-28 of

$$d = 4.6\ \eta^{1/4}\ \tilde{\nu}^{1/6}\ M_{1.4}^{1/6}\ I_{45}^{1/2}\ b^{1/2}\ R_6^{-1/2}\ \mathrm{kpc}, \tag{10}$$

where the geometric factor b depends on neutron-star parameters. By approximating the X-ray hot spot as a flat disk, we find $b \cong \cos\theta_{\rm obs} \cos\alpha$ in the limit $\theta_{\rm obs} + \theta_{\rm pc} + \alpha \ll \pi/2$ where neutron shadowing effects are unimportant. For 2-3 magnitudes of extinction per kpc in the direction of the Galactic Center, we estimate that the brightest optical counterpart would be at $V \cong 20 - 24$ for an M0 III giant ($M_V = -0.4$).

5. Discussion

GRO J1744-28 shows characteristics of both X-ray bursters and X-ray pulsars. Its intermediate magnetic field strength between the weak fields ($B \approx 10^{8-9}$ G) thought to reside in low-mass X-ray binaries and the strong fields ($B \approx 10^{12-13}$ G) found in X-ray pulsars suggests that its burst properties are related to those of X-ray bursters. But the relative fluences in the burst and persistent emissions probably rule out a thermonuclear origin in the initial bursting phase (Kouveliotou et al. 1996a; Strickman et al. 1996), although the energetics derived from *RXTE* observations (Swank et al. 1996) are favorable to such an interpretation. An accretion-disk instability seems implied by the similarity of the spectral shapes of the burst and persistent emission, since approximately equal energy per particle will be dissipated for an accretion-powered burst. We also note the similarities of the burst precursor and post-burst recovery period between the bursts from GRO J1744-28 and the Type II bursts of the rapid burster (compare Dotani et al. 1990; Lubin et al. 1992), the latter of which are thought to be due to accretion instabilities.

The beat-frequency model implies a testable relation between the persistent luminosity and the QPO centroid frequency given by equation (8). The inferred persistent luminosity implies a super-Eddington flux for the bursting episodes, since the burst flux is $\approx 2 - 8$ times as great as the persistent emission (Swank et al. 1996). The 3-5 minute recovery period following a burst observed by *RXTE* could be due to radiation effects on the disk.

The onset of detectable X-ray emission from this source cannot be due to orbital effects as in the case of Be X-ray binaries (the system is nearly circular with eccentricity $e < 0.026$; Finger et al. 1996b). We speculate that as the evolved companion expands and overflows its Roche lobe, the increased X-ray illumination drives an enhanced fueling episode (see Tavani & London 1993) which ceases when the heated atmosphere no longer overflows the

Roche surface. The star then contracts to a quiescent phase after which it resumes its slow expansion leading to the onset of another episode of mass transfer and luminous X-ray emission. Further calculations of evolution, accretion, and radiation will be required to yield a more complete understanding of this extraordinary system.

6. Acknowledgements

We thank Mark Finger, Eric Grove, Mike Harris, Chryssa Kouveliotou, Jim Kurfess, Gerry Share, Mark Strickman, Jean Swank, Marco Tavani, Bob Wilson, and Will Zhang for very useful discussions. This work was partially supported by the *Compton Gamma Ray Observatory* Guest Investigator Program GRO-95-135.

REFERENCES

Alpar, M. A., & Shaham, J. 1985, Nature, 316, 239

Briggs, M. S. , Harmon, B. A., van Paradijs, J., Kouveliotou, C., Fishman, G. J., Kommers, J., & Lewin, W. H. G. 1996, IAU Circ., No. 6290

Dotani, T. et al. 1990, ApJ, 350, 395

Finger, M. H., Wilson, R. B., Harmon, B. A., Hagedon, K., & Prince, T. A. 1996a, IAU Circ., No. 6285

Finger, M. H., Wilson, R. B., & van Paradijs, J. 1996b, IAU Circ., No. 6286

Fishman, G. J. et al. 1996, IAU Circ., No. 6290

Ghosh, P., & Lamb, F. K. 1979, ApJ, 234, 296

Kouveliotou, C., van Paradijs, J., Fishman, G. J., Briggs, M. S., Kommers, J., Harmon, B. A., Meegan, C. A., & Lewin, W. H. G. 1996a, Nature, in press

Kouveliotou, C., Kommers, J., Lewin, W. H. G., van Paradijs, J., Fishman, G. J., & Briggs, M. S. 1996b, IAU Circ., No. 6286

Lubin, L. M., Lewin, W. H. G., Rutledge, R. E., van Paradijs, J., van der Klis, M., & Stella, L. 1992, MNRAS, 258, 759

Mihalas, D., & Binney, J. 1981, Galactic Astronomy (San Francisco: Freeman)

Strickman, M. S., et al. 1996, ApJ, in press

Swank, J. et al. 1996, IAU Circ., No. 6291

Tavani, M., & London, R. 1993, ApJ, 410, 281

van der Klis, M. 1995, in X-Ray Binaries, ed. W. H. G. Lewin, J. van Paradijs, & E. P. J. van den Heuvel (Cambridge: Cambridge University Press), p. 252

Verbunt, F. 1990, in Neutron Stars and Their Birth Events, ed. W. Kundt (Dordrecht: Kluwer), 179

Wang, Y.-M. 1995, ApJ, 449, L153

Webbink, R. F., Rappaport, S., & Savonije, G. J. 1983, ApJ, 270, 678

Zhang, W. 1996, private communication

Zhang, W., Morgan, E., Swank, J., Jahoda, K., Jernigan, G., & Klein, R. 1996, IAU Circ., No. 6300

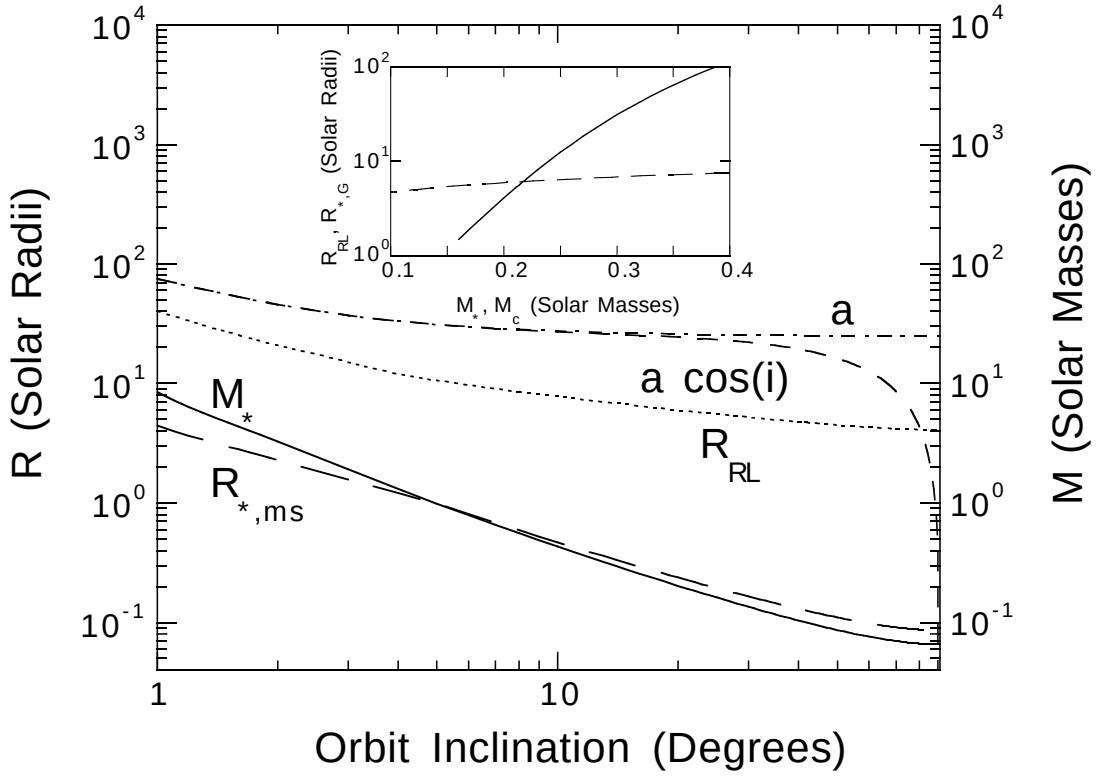

Fig. 1.— Relations between stellar masses and radii which are consistent with orbital parameters of GRO J1744-28. We plot the mean separation a, the mass of the stellar companion M_*, the main sequence radius $R_{*,\rm ms}$ of a stellar companion of mass M_*, and the average Roche lobe radius $R_{\rm RL}$ as a function of the orbital inclination angle i, assuming a 1.4 $M_\odot$ neutron star. If the companion fills its Roche lobe, the no-eclipse condition requires $a\ \cos(i) > R_{\rm RL}$. The inset shows the Roche lobe radius $R_{\rm RL}$ (dashed curve) as a function of M_* and the radius $R_{*,g}$ (solid curve) of an evolved companion as function of its helium core mass $M_{\rm c}$.

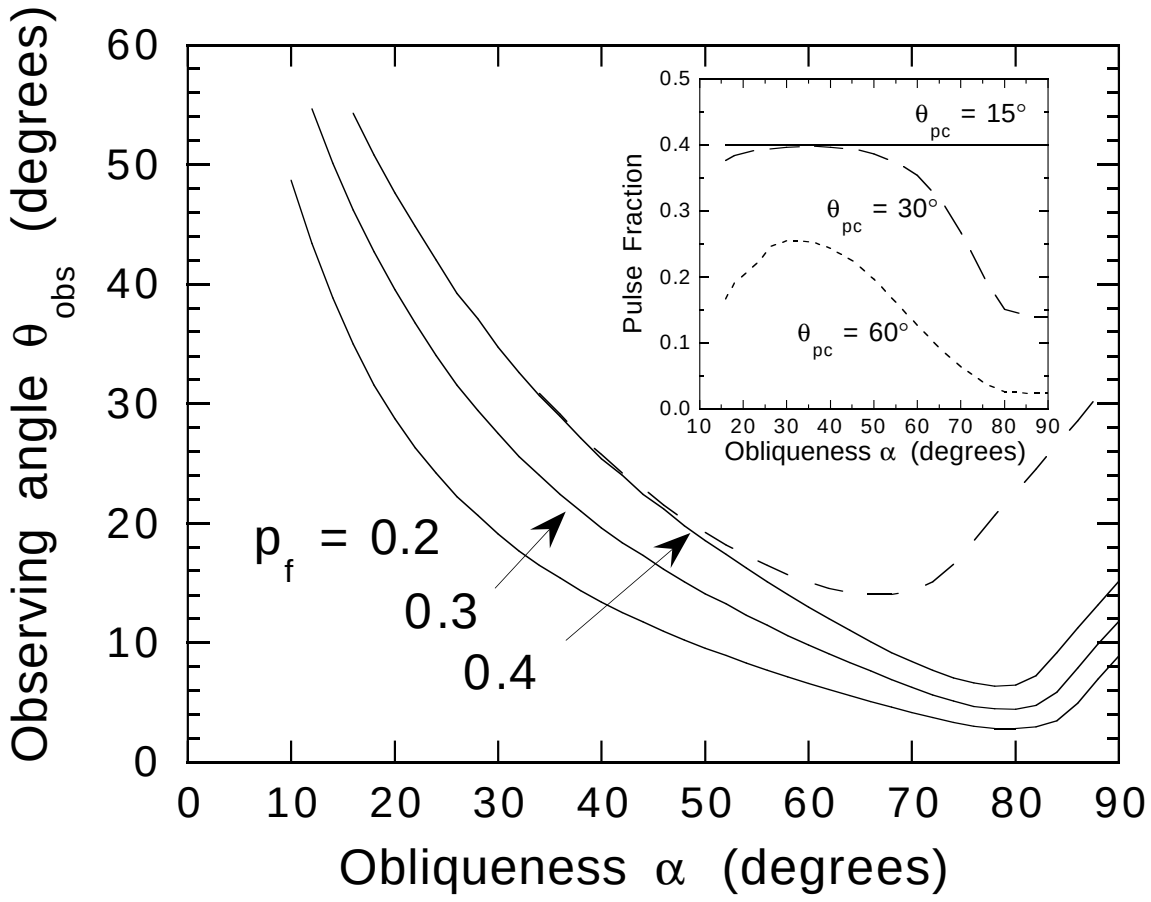

Fig. 2.— Values of α and $\theta_{\rm obs}$ giving pulse fractions $p_f = 0.2$, 0.3, and 0.4 for X-ray emitting hot spots with half-angle $\theta_{\rm pc} = 15°$ (solid curves) and 30° (dashed curve). The obliqueness α is the angle between the rotation and magnetic dipole axes, and θ_{obs} is the angle between the rotation axis and the direction to the line-of-sight. We define $p_f = (\phi_{\rm max} - \phi_{\rm min})/(\phi_{\rm max} + \phi_{\rm min})$, where $\phi_{\rm max(min)}$ represents the maximum (minimum) fluxes in the pulse profile. Inset shows variation of p_f for polar cap sizes $\theta_{\rm pc} = 30°$ and 60°, using values of α and $\theta_{\rm obs}$ which yield a 40% pulse fraction when $\theta_{\rm pc} = 15°$.